MAGNETIC RESONANCE IN CHEMISTRY
Magn. Reson. Chem. 2005; **43**: 231–234
Published online 8 December 2004 in Wiley InterScience (www.interscience.wiley.com). DOI: 10.1002/mrc.1521

Effects of static and dynamic perturbations on isotropic hyperfine coupling constants in some quinone radicals

S. L. Fiedler and J. Eloranta*

Department of Chemistry, University of Jyväskylä, PO Box 35, FIN-40351, Jyväskylä, Finland

Received 23 August 2004; Revised 8 October 2004; Accepted 14 October 2004

The effects of solvent dielectric response on the isotropic hyperfine coupling constants of the 1,4-benzoquinone, 1,4-naphthoquinone and 9,10-anthraquinone anions and 1,4-naphthalenediol cation radicals were studied by electron spin resonance (ESR) spectroscopy and by the theoretical density functional method within the polarizable continuum model. Experimental results demonstrate that the isotropic hyperfine coupling constants can be obtained with high accuracy and that the effects of solvent impurities can be minimized by careful sample preparation. The results obtained correlate well with theoretical predictions from density functional theory calculations. For 1,4-naphthalenediol both the solvent dielectric response as well as rotational averaging of the hydroxy groups were calculated. The overall results highlight the importance of static and dynamic perturbations to the couplings and aid in the assignation process of the couplings to specific magnetic nuclei. Copyright © 2004 John Wiley & Sons, Ltd.

KEYWORDS: ESR; quinone radicals; isotropic hyperfine couplings; dielectric solvent response

INTRODUCTION

Magnetic parameters of various quinone radicals have been studied extensively with electron paramagnetic resonance (EPR), electron–nuclear double resonance (ENDOR) and electron–nuclear–nuclear triple resonance (TRIPLE) spectroscopy-based methods.[1–4] These measurements have yielded information on both the magnitude and sign of the isotropic hyperfine coupling constants (IHCs). In some cases, it is possible to assign IHCs to particular magnetic nuclei trivially by considering the nuclear spin, or in more complicated cases through isotopic substitution. Generally, however, the molecules contain many nuclei of the same type and, especially for many quinones, consideration of nuclear spin alone is not sufficient. The isotopic substitution method is often quite laborious and therefore not a feasible approach. For these basic reasons, it is desirable to develop other methods that can be used for reliable assignation.

The semi-empicial quantum chemical method INDO (Intermediate Neglect of Differential Overlap) can be considered as the first practically applicable method able to aid in assignation of IHCs to specific magnetic nuclei, with qualitative agreement to experimental data for many organic radicals.[5] However, it often produced completely incorrect results, including IHCs for quinones, and therefore it could not be considered a reliable method.[6] *Ab initio* methods such as unrestricted Hartree–Fock typically produced results in even worse agreement with the experiments than INDO. Since then it has been recognized that accurate treatment of electron correlation as well as highly balanced basis sets are required to produce accurate values for IHCs in a vacuum.[7] Proper treatment of electron correlation is very expensive computationally and traditional configuration interaction approaches are not applicable to the relatively large quinone molecules with sufficiently large basis sets. In recent years density functional theory (DFT)-based methods have been shown to account for electron correlation to a sufficient extent and provide computational scaling similar to the Hartree–Fock method. Early calculations generated promising results using this approach[6] and since then more refined reports have appeared.[8] As the IHCs in quinone radicals tend to be closely spaced, it was important to consider contributions arising from the dielectric response of the solvent, possible counter-ions and rotational averaging.[9]

The objective of the current work is to report new results for the IHCs of the 1,4-benzoquinone anion, 1,4-naphthoquinone anion, 9,10-anthraquinone anion and 1,4-naphthalenediol cation radicals as a function of the solvent dielectric constant. Attention was paid towards producing dry solvents and thus minimizing the effects arising from possible hydrogen bonding of impurities such as water. The theoretical work considered both the dielectric solvent effects on the anion radicals as well as rotational averaging of the 1,4-naphthalenediol cation radical within the framework of electronic DFT. The present results provide direct comparison between the experimental and theoretical data.

EXPERIMENTAL

Electron spin resonance (ESR) spectra were measured with a Bruker ESP-300 series X-band spectrometer, employing

*Correspondence to: J. Eloranta, Department of Chemistry, University of Jyväskylä, PO Box 35, FIN-40351, Jyväskylä, Finland.
E-mail: eloranta@jyu.fi

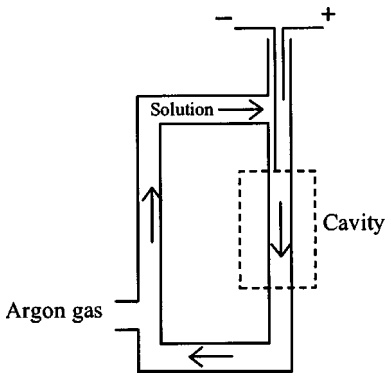

Figure 1. Schematic representation of the liquid flow cuvette. Liquid circulation prohibited excess argon gas from entering the measurement region inside the cavity.

12.5 or 100 kHz modulation frequencies and an modulation amplitude of <1 μT. In order to minimize power saturation effects, the incident power was <0.5 mW in all cases. Most of the measurements were carried out at room temperature using a closed-loop flow electrolysis cuvette driven by argon gas.[10] The radicals were produced by electrolysis with two platinum electrodes placed outside of the microwave cavity, as shown in Fig. 1. The supporting electrolyte (tetrabutylammonium iodide or tetrabutylammonium perchlorate) concentration was maintained at 0.1 mol dm^{-3}. To produce the anion radicals, the applied cell voltage (< 1.5 V) was increased gradually until the radical spectrum became observable via EPR. We estimate that the resulting radical concentrations were typically in the range of 10^{-4}mol dm^{-3}. Electrolytic measurements could not be carried out in dimethoxyethane (DME) due to technical problems in sample preparation. In this case, standard alkali metal reduction under high vacuum conditions with metallic sodium was used for producing the radicals.

The following chemicals were used as solvents: 1,2-dimethoxyethane (Riedel, >99%), dimehylsulphoxide (LAB-SCAN Analytical Sciences, 99.8%, DMSO), dimethylformamide (LAB-SCAN Analytical Sciences, 99.8%, DMF) and acetone (LAB-SCAN Analytical Sciences, 99.5%). Dimethoxyethane was dried with metallic sodium under vacuum and the other solvents were dried with Drierin ($CaSO_4$). The quinones were 1,4-benzoquinone (98%, Aldrich-Chemie), 1,4-naphthoquinone (Fluka, puriss.) and 9,10-anthraquinone (Fluka, purum). No further purification of these compounds was carried out. The supporting electrolytes were obtained as tetrabutylammonium iodide (Fluka) and tetrabutylammonium perchlorate (Sigma).

The IHCs were extracted from the experimental EPR spectra by an iterative simulation procedure as implemented in the xemr package.[11] In this procedure the root-mean-square (RMS) error between the experimental and the first-order simulated spectra is minimized with respect to the spectral parameters (i.e. IHC, g value and line width). Previously this procedure has been shown to give highly accurate results.[12] Provided that the lineshape function is known (e.g. Lorentzian) and a reasonable number of data points per spectral line are available, the accuracy of the IHCs generated ideally would by dependent only on experimental factors: magnetic field and microwave source stabilities and the signal-to-noise ratio. The limiting factor in the present study is the stability of the magnet ($\sim 10^{-6}$), which dictated our selection of 200 μT per data point resolution. Line width and overlap generate local minima and weak parameter dependencies in the RMS error function, thus increasing the difficulty in solving the global optimization problem. The minimization procedure itself does not directly yield error estimates for the parameters, however multiple optimization runs with different initial parameter values were used to obtain a qualitative gauge of the accuracy. For the results reported in this study, the accuracy was approximately the same as the spectral resolution.

COMPUTATIONAL DETAILS

The numbering schemes for the doublet-state quinone ion radicals are shown in Fig. 2. Geometry optimizations for the molecules were carried out within the SCIPCM polarizable continuum model (PCM)[13] at the B3LYP/6-31G* level.[14–17] Rotational barriers were calculated using rigid geometries, i.e. no geometry re-optimization was performed over variation of the torsional angle. The IHCs were extracted from single-point runs via the well-known Fermi contact analysis.[18] All calculations were performed with the Gaussian 03 package.[19]

Additional calculations were made for the 1,4-naphthalenediol cation radical where rotation of the hydroxyl groups contribute to the experimentally observed EPR spectrum. Owing to large out-of-plane zero-point motion and the thermal population of the rotationally excited states, the IHCs will experience deviations from their rigid geometry values. In this case, the EPR experiment observes rotationally averaged values of the IHCs.[9,20] For this work we assume that the two rotors (e.g. the two hydroxyl groups) are not coupled energetically and that the hydroxyl proton IHCs do not contribute to each other. This assumption reduces the dimensionality of the rotational problem from two to one. Furthermore, we have used only the rotational potential around the minimum geometry solution and ignored the other conformers ('cis 1' in Ref. 12; cf. Figure 2). This is a

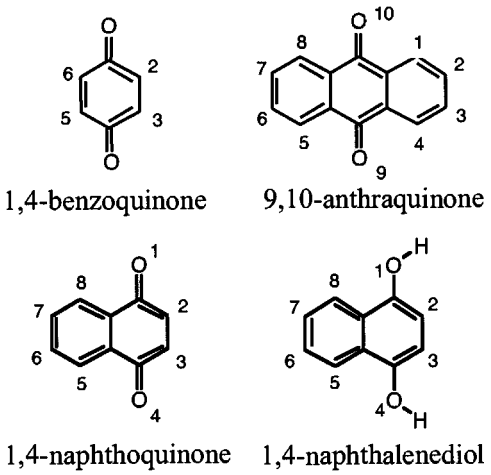

Figure 2. Numbering scheme for the relevant quinonone and quinol molecules.

valid assumption because the thermal population for the *cis* 1 state is ~98% under typical experimental conditions. The applied numerical procedure closely follows our previous work.[20]

RESULTS AND DISCUSSION

Experimental and computational results for 1,4-benzoquinone anion radical are shown in Fig. 3(a) and Table 1 as a function of the solvent dielectric constant. Apart from a constant offset, the experimental acetone, DMF and DMSO results follow the trend predicted by the DFT/SCIPCM calculations. For quinones, the performance of the theoretical dielectric solvent model depends essentially on its ability to model the solvent cavity in the vicinity of the quinone oxygens, which have large negative partial charges ($q \sim 0.6e$). For small values of the dielectric constant, changes in IHCs are pronounced but the experimental difficulty is also greater in this region. For example, the spectra obtained from the quinones in DME ($\varepsilon = 7.20$) contain large contributions from the sodium counter-ion (see Fig. 3(a)). Furthermore, in the high concentration limit of Na^+, the hyperfine structure due to the sodium nucleus can be seen clearly in the EPR spectra. Thus the resultant spectra are not representative of 'pure' anion/solvent systems. From a computational perspective, this type of counter-ion interaction cannot be modelled by PCM models but would require explicit consideration of the counter-ion in the calculation. The IHCs do, however, shift in the same direction for both cases (see Fig. 3(a)). Owing to the partial charges in water impurities, the IHCs are affected in the same way as for Na^+. Another signature for impurity interaction at the quinone oxygens is shown via an increase in the EPR spectral line width. These spectral signatures can be used as a sensitive probe for weak quinone oxygen interactions with its surroundings. Similar effects have been studied in more detail previously.[21] To address these concerns, experimentally it was essential to use very pure solvents and to carry out careful drying.

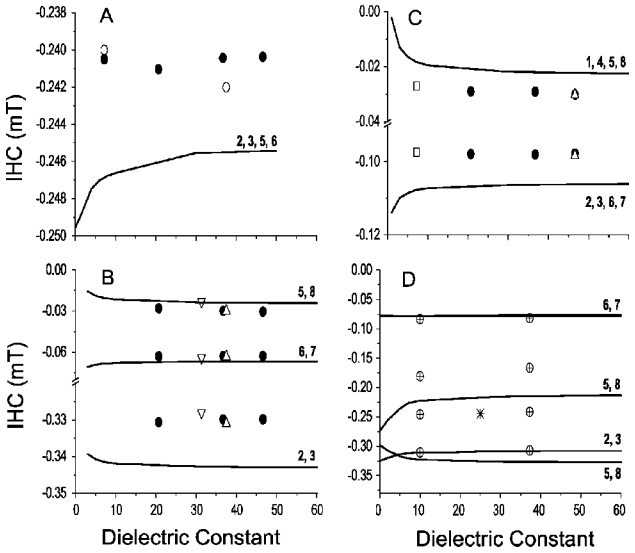

Figure 3. Dielectric response of the IHCs of 1,4-benzoquinone (A), 1,4-naphthoquinone (B) and 9,10-anthraquinone (C) anion radicals and 1,4-naphthalenediol cation radicals (D). The continuous line corresponds to simulated and symbols to experimental values. Experimental data were obtained from: (●) this work, (○) Ref. 2, (▽) Refs 22 and 23, (△) Ref. 3, (□) Ref. 4, (⊕) Ref. 12, (*) Fig. 5 (230 K). Positions of proton IHCs were identified according to Fig. 2. Solvents were: DME ($\varepsilon = 7.20$), acetone ($\varepsilon = 20.7$), DMF ($\varepsilon = 36.7$) and DMSO ($\varepsilon = 46.6$).

Table 1. Spectral parameters (mT) obtained from the iterative optimization procedure (results correspond to those shown in Fig. 3)

	Acetone	DMF	DMSO
ε	20.7	36.7	46.6
BQ line width	0.020	0.012	0.008
BQ IHC	−0.2410	−0.2404	−0.2404
NQ line width	0.012	0.006	0.004
NQ IHC(2,3)	−0.3306	−0.3298	−0.3298
NQ IHC(6,7)	−0.0630	−0.0628	−0.0627
NQ IHC(5,8)	−0.0279	−0.0298	−0.0303
AQ line width	0.013	0.008	0.006
AQ IHC(2,3,6,7)	−0.0979	−0.0980	−0.0978
AQ IHC(1,4,5,8)	−0.0291	−0.0292	−0.0302

A typical EPR spectrum of 1,4-naphthoquinone anion radical along with the simulated spectrum are shown in Fig. 4. Summaries of the experimental and theoretical results are plotted in Fig. 3(b). The smallest IHCs in magnitude follow the same trend as the DFT/SCIPCM-calculated values but the differences are very small and a reliable comparison is difficult to carry out. A small constant offset in the values originates from the applied DFT and basis set model. For the largest IHC, belonging to the protons at positions 2 and 3, the experimental and calculated results have opposite behaviour. However, the theoretical results appear consistent when compared with the case of 1,4-benzoquinone anion radical (cf. Figure 3(a)). The experimental EPR spectrum in acetone had larger line width (~ 0.012 mT) than in the other solvents (~ 0.004 mT). It was not possible to determine the origin of the line broadening because the present experimental set-up did not allow for variation of parameters such as temperature. This general trend in the line widths was observed for all quinone anions, with the largest widths in acetone and the smallest in DMSO (Table 1).

Results for 9,10-anthraquinone anion radical are shown in Fig. 3(c). For both DMSO and DMF solvents the slopes of the IHCs resemble the computed DFT/SCIPCM behaviour. The DMSO values, however, are not consistent, which is most likely due to the poor signal-to-noise ratio in the experimental EPR spectrum. Overall, the general trend matches the predictions from DFT/SCIPCM calculations. The ENDOR measurements could, in principle, be used to measure IHCs with better resolution than EPR but it was not straightforward to implement the electrolysis system, install the r.f. coils and vary the sample temperature all at the same time. As discussed previously, small amounts of residual water strongly affect the IHC at positions 1, 4, 5 and 8, and

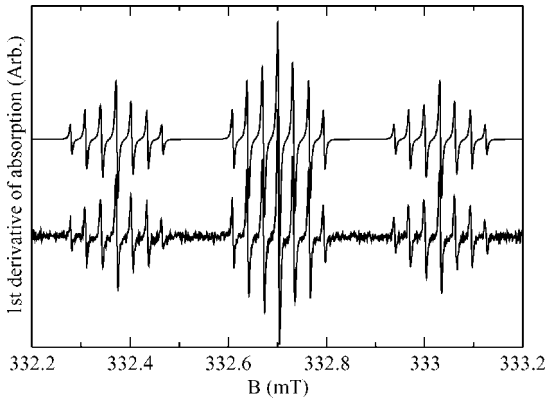

Figure 4. Experimental (bottom) and simulated (top) EPR spectra of 1,4-naphthoquinone anion radical in DMSO. The experimental spectrum was measured at room temperature with 1 μT modulation amplitude, 12.5 kHz modulation frequency and microwave power of 0.5 mW.

as such this signal could be used as a probe for any foreign species binding to the quinone oxygen.

We employed the 1,4-naphthalenediol cation radical as a prototype for considering dielectric solvent effects and accounting for both the thermal and zero-point (out-of-plane) motion of the hydroxyl groups. The effect of the dielectric solvent response on the IHCs is shown in Fig. 3(d). In a previous study, we generated the cation radical in strongly acidic solutions.[12] It was not straightforward, however, to extend this sample preparation method to other solvents with known dielectric constants, and electrolytic generation of cation radicals could not be achieved with the present cell set-up. We have indicated very approximate dielectric constants of the solutions (e.g. nitromethane and sulphuryl chloride fluoride) in Fig. 3(d), along with the experimental data. When out-of-plane motion of the hydroxyl was considered, the hydroxyl proton IHCs increased as a function of sample temperature (Fig. 5). The inset indicates the calculated rotational barrier. Consideration of non-zero temperature

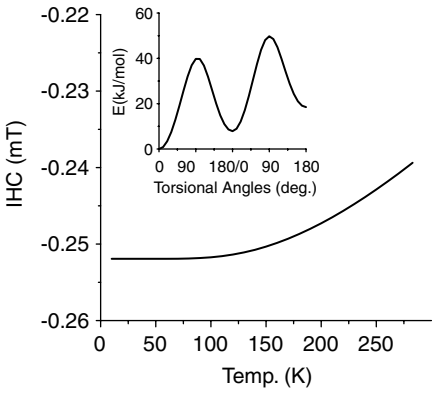

Figure 5. Temperature dependence of the hydroxyl proton IHC of 1,4-naphthalenediol. The inset displays the hydroxyl group rotational potential used for solving the torsional Schrödinger equation. The first, second and third minima correspond to *cis* 1, *trans* (7 kJ mol^{-1}) and *cis* 2 (17 kJ mol^{-1}), respectively. The experimental points correspond to Ref. 12.

(e.g. 250 K) brought the calculated hydroxyl proton IHC into agreement with the experimentally observed value.

High-resolution EPR spectroscopy combined with careful sample preparation methods were used to obtain information about the dielectric solvent response, quantum zero-point motion and thermal averaging processes. The present study notes the difficulty in producing clean aprotic samples, spectral line width limits of high-resolution EPR spectroscopy and sample preparation techniques. With these issues properly addressed experimentally, it was possible to compare directly the experimental data with DFT/PCM calculations. In the future we plan to extend the electrolysis system to our ENDOR spectrometer.

REFERENCES

1. Pedersen JA. *CRC Handbook of EPR Spectra from Quinones and Quinols*. CRC Press: New York, 1985.
2. Oakes J, Symons MCR. *Trans. Faraday Soc.* 1968; **64**: 2579.
3. Stone EW, Maki AH. *J. Chem. Phys.* 1962; **36**: 1944.
4. Das MR, Fraenkel GK. *J. Chem. Phys.* 1965; **42**: 1350.
5. Pople JA, Beveridge DL. *Approximate Molecular Orbital Theory*. McGraw-Hill: New York, 1970.
6. Eloranta J, Vatanen V, Grönroos A, Vuolle M, Mäkelä R, Heikkilä H. *Magn. Reson. Chem.* 1996; **34**: 898.
7. Chipman DM. *Theor. Chim. Acta* 1992; **82**: 93.
8. Langgärd M, Spanget-Larsen J. *J. Mol. Struct. (Theochem)* 1998; **431**: 173.
9. Improta R, Barone V. *Chem. Rev.* 2004; **104**: 1231.
10. Eloranta, J. *Doctoral Thesis*, University of Jyväskylä, Jyväskylä, Finland, 1997.
11. Eloranta J. *Electron Magnetic Resonance Software*, http://www.chem.jyu.fi/xemr, 2004.
12. Eloranta, J, Vuolle M. *Magn. Reson. Chem.* 1998; **36**: 98.
13. Foresman JB, Keith TA, Wiberg KB, Snoonian J, Frisch MJ. *J. Chem. Phys.* 1996; **100**: 16 098.
14. Becke AD. *J. Chem. Phys.* 1993; **98**: 5648.
15. Vosko SH, Wilk L, Nusair M. *Can. J. Phys.* 1980; **58**: 1200.
16. Lee C, Yang W, Parr RG. *Phys. Rev. B* 1988; **37**: 785.
17. Gordon MS. *Chem. Phys. Lett.* 1980; **76**: 163.
18. McWeeny, R. *Methods of Molecular Quantum Mechanics* (2nd edn). Academic Press: London, 1992.
19. Frisch MJ, Trucks GW, Schlegel HB, Scuseria GE, Robb MA, Cheeseman JR, Montgomery JA, Vreven T, Kudin KN, Burant JC, Millam JM, Iyengar SS, Tomasi J, Barone V, Mennucci B, Cossi M, Scalmani G, Rega N, Petersson GA, Nakatsuji H, Hada M, Ehara M, Toyota K, Fukuda R, Hasegawa J, Ishida M, Nakajima T, Honda Y, Kitao O, Nakai H, Klene M, Li X, Knox JE, Hratchian HP, Cross JB, Adamo C, Jaramillo J, Gomperts R, Stratmann RE, Yazyev O, Austin AJ, Cammi R, Pomelli C, Ochterski JW, Ayala PY, Morokuma K, Voth GA, Salvador P, Dannenberg JJ, Zakrzewski VG, Dapprich S, Daniels AD, Strain MC, Farkas O, Malick DK, Rabuck AD, Raghavachari K, Foresman JB, Ortiz JV, Cui Q, Baboul AG, Clifford S, Cioslowski, J, Stefanov BB, Liu G, Liashenko A, Piskorz P, Komaromi I, Martin RL, Fox DJ, Keith T, Al-Laham MA, Peng CY, Nanayakkara Challacombe AM, Gill PMW, Johnson B, Chen W, Wong MW, Gonzalez C, Pople JA. *Gaussian 03, Revision B.2*. Gaussian,: Pittsburgh, PA, 2003.
20. Eloranta J, Suontamo R, Vuolle M. *J. Chem. Soc. Faraday Trans.* 1997; **93**: 3313.
21. Vatanen V, *Doctoral Thesis*, University of Jyväskylä, Jyväskylä, Finland, 2000.
22. Stevenson, GR, Alegria AE, Block AMcB. *J. Am. Chem. Soc.* 1975; **97**: 4859.
23. Dixon, WT, Murphy D. *J. Chem. Soc. Perkin Trans.* 1974; **2**: 1430.